Environmental Pollution 308 (2022) 119627

Contents lists available at ScienceDirect

Environmental Pollution

journal homepage: www.elsevier.com/locate/envpol

Large-scale sampling of the freshwater microbiome suggests pollution-driven ecosystem changes☆

Katrin Premke [a,b,*], Christian Wurzbacher [c], Katja Felsmann [a], Jenny Fabian [d], Robert Taube [e], Pascal Bodmer [f], Katrin Attermeyer [g,h], Kai Nils Nitzsche [i], Sibylle Schroer [a], Matthias Koschorreck [j], Eric Hübner [a], Termeh Hesam Mahmoudinejad [c], Christopher C.M. Kyba [a,k], Michael T. Monaghan [a,l], Franz Hölker [a,l]

[a] Leibniz Institute of Freshwater Ecology and Inland Fisheries (IGB), Berlin, Germany
[b] Charité–Universitätsmedizin Berlin, Berlin, Germany
[c] Technical University of Munich (TUM), Munich, Germany
[d] Leibniz Institute for Baltic Sea Research Warnemünde (IOW), Rostock, Germany
[e] City University of Applied Science, Bremen, Germany
[f] Université du Québec à Montréal, Montreal, Canada
[g] WasserCluster Lunz - Biologische Station, Lunz am See, Austria
[h] Department of Functional and Evolutionary Ecology, University of Vienna, Vienna, Austria
[i] Japan Agency for Marine-Earth Science and Technology (JAMSTEC), Yokosuka, Japan
[j] Helmholtz Centre for Environmental Research (UFZ), Magdeburg, Germany
[k] GFZ German Research Centre for Geosciences, Helmholtz Centre, Potsdam, Germany
[l] Institute für Biologie, Freie Universität Berlin, Berlin, Germany

ARTICLE INFO

Keywords:
Microbial diversity
Antibiotic-resistance genes
Artificial light at night
Carbon dioxide
Citizen science
Climate change

ABSTRACT

Freshwater microbes play a crucial role in the global carbon cycle. Anthropogenic stressors that lead to changes in these microbial communities are likely to have profound consequences for freshwater ecosystems. Using field data from the coordinated sampling of 617 lakes, ponds, rivers, and streams by citizen scientists, we observed linkages between microbial community composition, light and chemical pollution, and greenhouse gas concentration. All sampled water bodies were net emitters of CO_2, with higher concentrations in running waters, and increasing concentrations at higher latitudes. Light pollution occurred at 75% of sites, was higher in urban areas and along rivers, and had a measurable effect on the microbial alpha diversity. Genetic elements suggestive of chemical stress and antimicrobial resistances (*IntI1*, $blaOX_{58}$) were found in 85% of sites, and were also more prevalent in urban streams and rivers. Light pollution and CO_2 were significantly related to microbial community composition, with CO_2 inversely related to microbial phototrophy. Results of synchronous nationwide sampling indicate that pollution-driven alterations to the freshwater microbiome lead to changes in CO_2 production in natural waters and highlight the vulnerability of running waters to anthropogenic stressors.

1. Introduction

The important functional role of freshwater microorganisms in the global carbon cycle is well established (Whitman et al., 1998; Raymond et al., 2013; Crevecoeur et al., 2019; del Giorgio and Duarte, 2002). They are responsible for most of the uptake and emission of greenhouse gases (GHGs) in freshwaters including carbon dioxide (CO_2) and methane (CH_4) (Aufdenkampe et al., 2011), and their impact on net carbon balance has direct effects on climate and global change (Gudasz et al., 2010). Ecosystem changes, many of which result from human activities, are increasingly perturbing global carbon cycles (Regnier et al., 2013), in turn hampering our understanding of related processes and limiting the predictability of Earth System Models (Verburg et al., 2016). A recent "warning to humanity" highlighted the urgency of improving our understanding of how microorganisms regulate GHG dynamics, and how this function will be modulated by human activities

☆ This paper has been recommended for acceptance by Sarah Harmon.

* Corresponding author. Charité–Universitätsmedizin Berlin, Berlin, Germany.
E-mail address: katrin.premke@charite.de (K. Premke).

https://doi.org/10.1016/j.envpol.2022.119627
Received 17 December 2021; Received in revised form 10 June 2022; Accepted 12 June 2022
Available online 14 June 2022

(Cavicchioli et al., 2019).

The freshwater microbiome has been extensively studied, with a focus on linking bacterial community structure to local physicochemical properties of water. The majority of studies have been conducted in temperate lakes or streams, and broader geographical studies across different waterbody types are sparse (Veach et al., 2021). Existing studies also focus on bacteria and rarely extend to the complete freshwater microbiome which includes archaeal and eukaryotic microbes (Wurzbacher et al., 2017). While freshwater microbial communities can be similar in different habitats, there can be notable differences among types of water body, as commonly observed for phytoplankton and microbial eukaryotes (da Silva et al., 2019; Reynolds et al., 1994). It is likely that these differences also extend to prokaryotes and thus influence microbial production and mineralization. Freshwater ecosystems are a significant source of microbially mediated CO_2 and CH_4 (Raymond et al., 2013; Tranvik et al., 2009) and transform a large amount (up to 5.1 Pg C y^{-1}) (Bretz et al., 2021) of the terrestrial carbon sink. In addition to water-column processes of the plankton, microorganisms living in sunlit (i.e., euphotic) sediments are important for the assimilation of CO_2 through photosynthesis and the release of CO_2 and CH_4 through mineralization (i.e., primary production and respiration). CO_2 concentration in freshwaters can also be influenced by the import of carbon from the adjacent landscape (Bretz et al., 2021). CH_4 is mainly produced by methanogenic archaea in sediments as an end product of anaerobic decomposition of organic matter. It is also produced as a result of cellular stress under oxic conditions (Ernst et al., 2022). CH_4 can be removed from the system by e.g., methane oxidizing bacteria (MOBs) once an electron acceptor is available. Together, CO_2 and CH_4, account for approximately 75% (Drake et al., 2018) of all carbon metabolism in inland waters. These freshwaters are increasingly subject to modification and degradation by anthropogenic stressors, with the highest global species extinction rates of any biome and with eutrophication from nutrient pollution a decades-old problem (Reid et al., 2019). This is despite the high value of freshwaters for recreation and conservation and their contribution to human health and well-being (Venohr et al., 2018).

Two emerging and diffuse anthropogenic stressors in freshwaters are closely linked to urbanization: light pollution in the form of artificial light at night (ALAN) (Hölker et al., 2010; Kyba et al., 2017) and the spread of chemical pollution such as antibiotics (Amos et al., 2014; Bengtsson-Palme and Larsson, 2015). Light pollution can affect organism and nutrient fluxes across ecosystem boundaries (Manfrin et al., 2017) and can change microbial community composition (Grubisic et al., 2017), favouring taxa that benefit from nocturnal light and potentially leading to altered carbon budgets (Hölker et al., 2015). Chemical pollution can lead to the spread of resistance genes in the environment (Amos et al., 2014, Bengtsson-Palme and Larsson, 2015), perhaps through selection pressure exerted by the extensive use of antimicrobial agents. Prominent transfer routes to freshwaters may be via manure-fertilized agriculture (Lima et al., 2020), polluted road runoff (Liguori et al., 2021), or wastewater treatment infrastructure (Amos et al., 2014; Cacace et al., 2019). Transfer can lead to the spread of mobile genetic elements (e.g., integron integrase genes) that serve as biomarkers for presence of antibiotics, heavy metals, and disinfectants present in anthropogenic pollution (Gillings et al., 2015). While ALAN can be directly measured in the field or by remote sensing (Jechow & Hölker, 2019), chemical pollution can be indirectly assessed by the presence of the mobile class 1 integron-integrase gene. The ecological effects of these types of pollution on microbial communities have been studied with small-scale experiments, but our understanding of the effects at the landscape level or larger spatial scales is limited, despite the fact that these stressors are likely to have manifold effects on aquatic ecosystems (Hölker et al., 2021).

We investigated the linkages between benthic microbial community composition and two emerging pollutants, light pollution and chemical pollution, by initiating a nationwide sampling event in Germany in November 2015. Light pollution was studied directly as artificial light at night, while chemical pollution was studied indirectly using integron-integrase genes as biomarkers. In total, 742 individuals and groups of citizen scientists sampled 617 sites that encompassed ponds, lakes, streams, and rivers in a two-week period. Our set-up allowed us to test four hypotheses: (i) light pollution is more evident in urban areas while biomarkers of chemical pollution are more pronounced in agricultural areas, (ii) light pollution has an impact on sediment microbial community composition, (iii) these effects on microbial communities by light pollution can lead to alterations in the carbon cycle, here measured as GHG concentrations, and (iv) differences in microbial community composition can be linked to the type of water body.

2. Materials and methods

A total of 280 lakes (>0.01 km^2), 71 ponds (standing water <0.01 km^2), 105 rivers (stream order 7–10), and 161 streams (stream order 1–6, Fig. S1) were surveyed by conducting a citizen science sampling campaign throughout Germany.

2.1. Citizen science field sampling

The citizen science field sampling campaign was conducted in the first two weeks in November 2015. Citizens were invited to register online using an interactive inland water map that indicated the registered locations and, later, the successful return of the sample and information about the respective freshwater system. A sampling kit was sent to registered participants. The kit contained three glass vials (21 ml) for taking water samples, a 5-ml syringe (Carl Roth GmbH, Karlsruhe, Germany) with tip cut off for taking sediment samples, a 15-ml centrifuge tube (Carl Roth) containing RNA stabilizing solution (RNAlater, Invitrogen Thermo Scientific, Waltham, USA) into which 1 ml of sediment from the 5-ml syringe was added immediately after each sample was taken, a thermometer, pH-measuring paper, gloves, a pencil, a logbook, and a detailed manual with a link to an online video tutorial for sampling of water and sediment (https://www.youtube.com/watch?v=2AumuRLgimo). The participants were asked to take samples at a freshwater body close to their home. A questionnaire about the local illumination was added to the kit, asking for (a) the distance from the sampling site to the nearest light source, (b) the number of the visible light sources from the sampling site, (c) the estimated light color of the most visible light sources, and (d) details about the design and condition of artificial light sources (Schroer et al., 2016).

In total, 742 sampling kits were sent to registered citizens and organizations. Participants recorded the exact time and location of the sampling (using Google Maps GPS data) and other sampling metadata. All samples were taken between 7:00–10:00 (Central European Standard Time), while the light exposure was examined after 18:00 (Central European Standard Time) to ensure darkness. Citizen scientists took three water samples and one sediment sample per sampling site. Temperature, light, and pH were measured in situ. Sediment samples were taken from the uppermost few cm of sediment (i.e., benthos) in an area where water depth was about 30 cm and transferred into the prepared RNAlater vials. Water and sediment samples were sent by post to the Leibniz Institute of Freshwater Ecology and Inland Fisheries (IGB) by participants, having been stored at most for two days in a home refrigerator (<7 °C). After arrival at IGB, the samples were immediately measured or were stored at 4 °C until further processing (see following sections).

The project required an extensive involvement of citizens throughout Germany who may be subject to spatial bias, in particular through the addition of variability to the data and by a non-randomized sampling design (Kyba et al., 2013). The impact of the noise introduced by citizen science methodologies can be assessed by validating previously observed patterns on a large citizen science-based dataset. By comparing and confirming our results with an expected pattern, here a higher CO_2 concentration in small waters compared to large ones (Holgerson and

Raymond, 2016; Premke, 2016), we validated that the citizen science approach of our study is a powerful tool for intensive synchronous data collection along a wide geographic range and in different sampling sites.

2.2. Biomolecular analysis of the microbial community

Microbial communities from preserved sediment samples were analysed using DNA metabarcoding of the ribosomal SSU (Wurzbacher et al., 2017), and indicators for chemical pollution and antibiotic resistance were measured via quantitative PCR. DNA was extracted from samples (1 ml sediment per site) stored in RNALater using ZR-96 Soil Microbe DNA Kits (Zymo Research Europe GmbH, Freiburg, Germany). Samples were first washed with 1.5 ml PBS and centrifuged (5000xg for 10 min, 4 °C) to remove the RNALater. Approximately 150 μl of washed sediment was then suspended in a lysis buffer and extracted according to the manufacturer's protocol. In total, 567 benthic samples were successfully extracted. A fragment of ribosomal SSU was PCR-amplified with two equimolar 926F primers that contained a two-base pair shift to mitigate phasing effects, and two equimolar 1392R primers (see supplementary material). Primers were adapter-ligated using the Nextera library preparation protocol (Illumina, San Diego, USA, see supplementary material). For this first adapter PCR we used the Herculase II Fusion DNA Polymerase (Agilent Technologies Germany GmbH, Waldbronn, Germany) in a hot start PCR in 20 μl reactions (with 18 μg of molecular grade BSA added per reaction). We used an initial denaturation at 95 °C (3 min) followed by 25 cycles of 95 °C (30 s), 55 °C (45 s), 70 °C (90 s), and a final elongation at 72 °C (5 min). PCR products were checked for successful amplification on an agarose gel (1%). The amplicons were purified with 1 volume of AMPure XP magnetic beads (Beckman Coulter GmbH, Krefeld, Germany) and subsequently amplified in a second index PCR using the Nextera index primers N701–N724 and S501–S516 (Illumina, Nextera index primer) with the Q5 High-Fidelity Polymerase (New England Biolabs, Ipswich, USA) in a hot-start PCR reaction of 20 μl. The PCR conditions consisted of denaturation at 98 °C (1 min), 10 PCR cycles of 98 °C (10 s), 66 °C (30 s), 72 °C (30 s), and a final elongation at 72 °C (2 min). PCR products were purified with magnetic beads as described above and DNA concentration was measured using the Quant-iT PicoGreen dsDNA Assay-Kit (Invitrogen Thermo Scientific). Randomly selected samples from the first and second PCR were qualitatively analysed on a Bioanalyzer (Agilent Technologies). Two of the 96 well plates containing the barcoded amplicons were equimolar pooled and purified with magnetic beads. The final pool was analysed on a Bioanalyzer (Agilent Technologies) prior to sequencing on a MiSeq sequencer (Illumina) with a v3 chemistry (2 × 300 nt). Data were retrieved after basecalling as sample-based fastq files. Reads were trimmed with Trimmomatic (Bolger et al., 2014) and merged with Pear (Zhang et al., 2014), translated into fasta files, and subjected to the closed-reference SILVA NGS pipeline (https://ngs.arb-silva.de/silvangs/) for processing, resulting in a community matrix resolved to the genus level (Quast et al., 2013). The community matrix was screened for artificial signals related to low DNA concentrations (Salter et al., 2014) by correlations (threshold of $r = 0.3$) and the following taxa were identified and removed from the dataset: Mammalia, *Mycoplasma*, *Rhodococcus*, *Propionibacterium*, *Curvibacter*, *Ralstonia*; reported frequent contaminants in metabarcoding studies (Salter et al., 2014). This resulted in a total of 4733 taxonomic paths (Quast et al., 2013). To test whether there were single-species-like effects of artificial light at night we processed the sequence data using the data processing pipeline presented in Nawaz et al. (2018) with small modifications, setting the SILVA SSU database as reference (SILVA version 138), resulting in a community matrix on the OTU level (corresponding to genus or species for most OTUs).

2.3. Genetic markers for chemical stress: Intl1 and blaOXA$_{58}$ analyses

The antibiotic resistance gene and the class 1 integron integrase gene (*blaOXA*$_{58}$ Cacace et al., 2019, *intl1* (Barraud et al., 2010)) were quantified by quantitative PCR normalized to per-sample 16S gene copies using the primers 337f/518r (Bakke et al., 2011). Standard curves were generated by linearized plasmid (for 16S gene) or by double magnetic bead purified PCR products from wastewater (municipal wastewater treatment plant Garching, Germany) using MagSi-NGSPREP Plus (Steinbrenner, Magtivio, Nuth, Netherlands) according to the manufacturer's protocol. Quantification was done in the QFX Fluorometer (DeNovix, Wilmington, USA) using the Qubit dsDNA BR Assay Kit (Thermo Fisher Scientific). All steps were quality-checked on agarose gels. Serial dilutions were generated by 10-fold dilutions and measured together with the samples in technical replicates. The PCR was performed with SybrGreen GoTaq qPCR master mix (Promega, Madison, USA) in 21 μl reactions in a CFX96 thermocylcer (Bio-Rad Laboratories, Berkeley, USA). The qPCR was run with following conditions for *intl1* and *blaOXA*$_{58}$: Initial denaturation at 95 °C for 4 min, and then 40 cycles (95 °C for 10 s followed by 64 °C (*Intl1*) or 60 °C (*blaOXA*$_{58}$) for 45 s). For 16S we used an initial denaturation at 95 °C for 2 min, and then 40 cycles (95 °C for 5 s, 60 °C for 30 s). All qPCRs were followed by a melt-curve analysis and samples with secondary signals were removed from the analysis. To test the relevance of the geographical proximity to the nearest upstream wastewater treatment plant, we identified the nearest neighbour using the distance matrix tool in QGIS (version 2.14.22) and calculated the distance. For this purpose, the studied points geospatial data were defined as the input point layer and the WWTP geospatial data as the target point layer.

2.4. Artificial light at night (ALAN)

Emissions of night-time light in the wavelength range 500–900 nm were assessed using cloud- and moon-free data from the Visible Infrared Imaging Radiometer Suite Day/Night Band (DNB) for the month of November 2015 (https://eogdata.mines.edu/download_dnb_composites.html).

2.5. Measurement and calculation of dissolved CO_2 and CH_4 concentrations

To assess the concentrations of the GHGs CO_2 and CH_4 in the water, unpreserved surface water samples were analysed in the laboratory using the headspace extraction technique (Kling et al., 1991). Vials (21 ml) were filled by citizen scientists under water, closed with butyl rubber stoppers and screw caps, and stored in a refrigerator until shipment to the laboratory. The measurement for dissolved CH_4 and CO_2 concentration was carried-out by creating a 5-ml gas headspace with atmospheric air and equilibrating the water and the headspace gas by rigorously shaking the vial for 1 min. The concentration of CH_4 and CO_2 in the headspace gas was then measured by injecting a 1 ml subsample of the gas headspace with a glass gas-tight syringe (Hamilton 1710RN, Switzerland) in a closed-loop connected to an Ultraportable Greenhouse Gas Analyzer (UGGA, Los Gatos Research Inc, Mountain View, USA) (Kling et al., 1991; Attermeyer et al., 2016; Wilkinson et al., 2019). About 13% of the samples were analysed by a gas chromatograph equipped with an FID and methanizer (SRI 8610C, SRI-Instruments, Torrance, USA). Both instruments were adjusted and calibrated to each other. The equilibration temperature (i.e., water temperature) was measured in the first and last vial of each 3-sample batch. The dissolved CO_2 and CH_4 concentrations, corrected for the moles of CO_2 and CH_4 in the atmospheric air introduced to create the headspace, were determined according to Baird et al. (2010), using the equilibration temperature-adjusted solubility constants according to Sander (1999).

2.6. Calculations of Strahler stream orders

Strahler stream order was determined for each lotic sampling site in three steps. First, analysed areas were restricted by delineating

watersheds of investigated streams using the location of the sampling sites, the low-resolution flow direction (HydroSHEDS) (Lehner et al., 2008) and a flow accumulation raster. Second, stream networks were reconstructed on delineated areas with stream source points (extracted from the Authorative Topographic-Cartographic Information System (ATKIS®) data set (© GeoBasis-DE/German Federal Agency for Cartography and Geodesy - BKG) (2013)) and the HydroSHEDS[4] high-resolution flow direction raster, using a System for Automated Geoscientific Analysis (SAGA) (Conrad et al., 2015) tool and an optimized procedure for digital elevation model analysis. Finally, Strahler stream orders were computed based on the reconstructed stream network. The optimized procedure is similar to those used in contemporary GIS software for digital elevation model analysis. Inputs of the procedure are flow direction raster and initiation grid.

2.7. Additional analyses

We performed two additional analyses to (1) estimate possible changes in GHG concentration during storage and transport of the GHG vials and to (2) examine the geographical distribution of the sampled water bodies. All details are given in the supplementary material. Briefly, during storage, microbial activity can affect the concentration of CO_2 and CH_4 in water samples. This effect increases with temperature and time of storage. To quantify any time and temperature effects we used an additional experiment in the laboratory. We stored lake water for three time-periods at two different temperatures (4 °C, 15 °C), which corresponds to the conditions of sample storage in our citizen science study. When stored at 4 °C, there was no significant change in the GHG concentrations over 5 days. Moreover, the storage effect remained small when samples were stored at 15° over 5 days (Table S1). We thus conclude that the length of time between sampling and analysis had no significant effect on the measured GHG concentrations, because vials were stored at 4 °C for most of the storage time.

Furthermore, we gathered information about absolute numbers of water bodies from environmental authorities from the federal states of Germany to compare them to the coverage of the sampled water bodies in this study. The sampled water bodies covered about 0.25% of all lentic water bodies, with the coverage per federal state ranging from 0.02 to 0.4% (Table S2). The highest coverage was in Nordrhein-Westfalen followed by states near Berlin (Brandenburg, Mecklenburg-Vorpommern). Comparing the size of the sampled standing water bodies, we recognized a skewed distribution towards larger water bodies. Hence, the selection of the water bodies by the citizen scientists was influenced by recruitment that was more successful close to the coordinating research institute in Berlin (IGB) and had a tendency towards larger water bodies. However, we consider this negligible for the interpretation of our data.

2.8. Statistical analyses

All statistical analyses of microbial community and greenhouse gas data were performed in R (R Core Team, 2018) v 4.0.2. To assess the diversity of the benthic microbial community and the influence of the environmental stressors and other parameters, richness estimates of the microbial community were calculated as Hill numbers (Raymond et al., 2008) using the iNEXT package (Hsieh et al., 2016), with a sample coverage of 0.9 using the microbial community matrix from the SILVA NGS pipeline. The following multivariate analyses including microbial community were performed using the vegan (Oksanen et al., 2007) package with Bray-Curtis distances. We first rarefied all samples at 5000 reads which resulted in 487 sites after rarefaction. The adonis (sequential model) and adonis2 (marginal model and overall model (AKTIS, 2013) functions were applied for calculating the influence of the predictor variables in a strength based order using 9999 permutations on the microbial community matrix using Bray Curtis distances. With these analyses, we were able to investigate the impact of the two emerging pollutants on the surface microbial community composition according to the aims formulated here. The Mantel test was used to calculate spatial autocorrelations. To specifically test whether CO_2 could be considered a response of the microbial community composition and, hence, if there is a feedback on the carbon cycle, we used a random forest model using the function randomForest (Liaw and Wiener, 2002). An NMDS was calculated using the metaNMDS function and the fitting of environmental factors and categorical parameters to the two-dimensional plot was done using the function envfit with a significance cutoff of $P = 0.010$. The correlation analysis was done using the script from the Rhea collection (Lagkouvardos et al., 2017) and a higher resolution community matrix rarefied to 9000 reads per sample resulting in 441 samples. Two random variables were included to confirm the correlation cutoffs (n = 50%, P adjusted <0.050, and R > 0.2). The plots were generated with the packages phyloseq (McMurdie & Holmes, 2013), ggplot2 (Villanueva & Chen, 2019) (v. 3.2.2), and microbiome (http://microbiome.github.io/microbiome/).

Furthermore, we used linear models to simultaneously test for effects of latitude, longitude, water body type (lake, pond, river, stream), and dominant land use within a 0.5-km radius of the sampling site (arable land, forest, grassland, open-pit mining, urban area, water area, wetland) on the response variable CO_2 or CH_4 concentration in surface water using the lme4 package (Bates et al., 2015)) (loge transformed; two separate models). Latitude, longitude, and water body type were included as fixed effects. We tested for the potential interaction between fixed effects, and the statistical significance of each, using a likelihood ratio test to compare models with and without the effect.

We tested for changes in CO_2 with Strahler stream order and for variations in ALAN and *Intl1* among water body types relative to their catchment using linear models. Elevation data originated from a digital terrain model based on data from the Shuttle Radar Topography Mission and OpenStreetMap (OpenStreetMap, 2018). All linear model analyses were followed by a model validation, checking the residuals for normal distribution and homogeneity of variances. Post-hoc tests of water-body type and dominant land use were performed with the TukeyHSD function in the mosaic package (Pruim et al., 2017). Ordinary Kriging on CO_2 (<1000 μmol L^{-1}) was conducted using ArcGIS 10.8 (AKTIS, 2013) after detecting a weak spatial autocorrelation of CO_2 (Moran's I = 0.085, $P <$ 0.001).

3. Results and discussion

3.1. Freshwater microbiome

Microbial community richness (as Hill diversity, D: exponential of Shannon entropy) ranged from 17 to 312 per site (Fig. 1c) and the citizen science sampling yielded a taxonomic composition that is typical of inland freshwaters and sediments (Wan et al., 2017) and that separated into slightly different core microbiomes (Fig. 3, Fig. S2). We are aware of very few studies that have examined euphotic sediments (Han et al., 2020) and ours is one of the first systematic treatments of euphotic sediments across a wide range of freshwater ecosystems. Surface-sediment community composition varied among water body types, with more phototrophic Cyanobacteria lineages in lakes and more Actino- and Acidobacteria in streams and rivers (Fig. 3). Composition exhibited only a weak spatial autocorrelation (Mantel test, $R^2 = 0.04$, $P = 0.013$), pointing to greater role of environmental filtering in determining composition. Fitting all parameters to two-dimensional nonmetric multi-dimensional scaling (NMDS) in a simplified model revealed a collinearity of urban area, *intI1*, and light pollution (Fig. 3). A multivariate model indicated that microbial communities were mostly linked to CO_2 and the type of water body, supporting our fourth hypothesis. Longitude, latitude, land use, and CH_4 played less important roles (Table S2). This was confirmed by a non-linear random forest analysis with microbial taxa as predictors that explained 30% of CO_2 variation, and which was consistent with a large number of

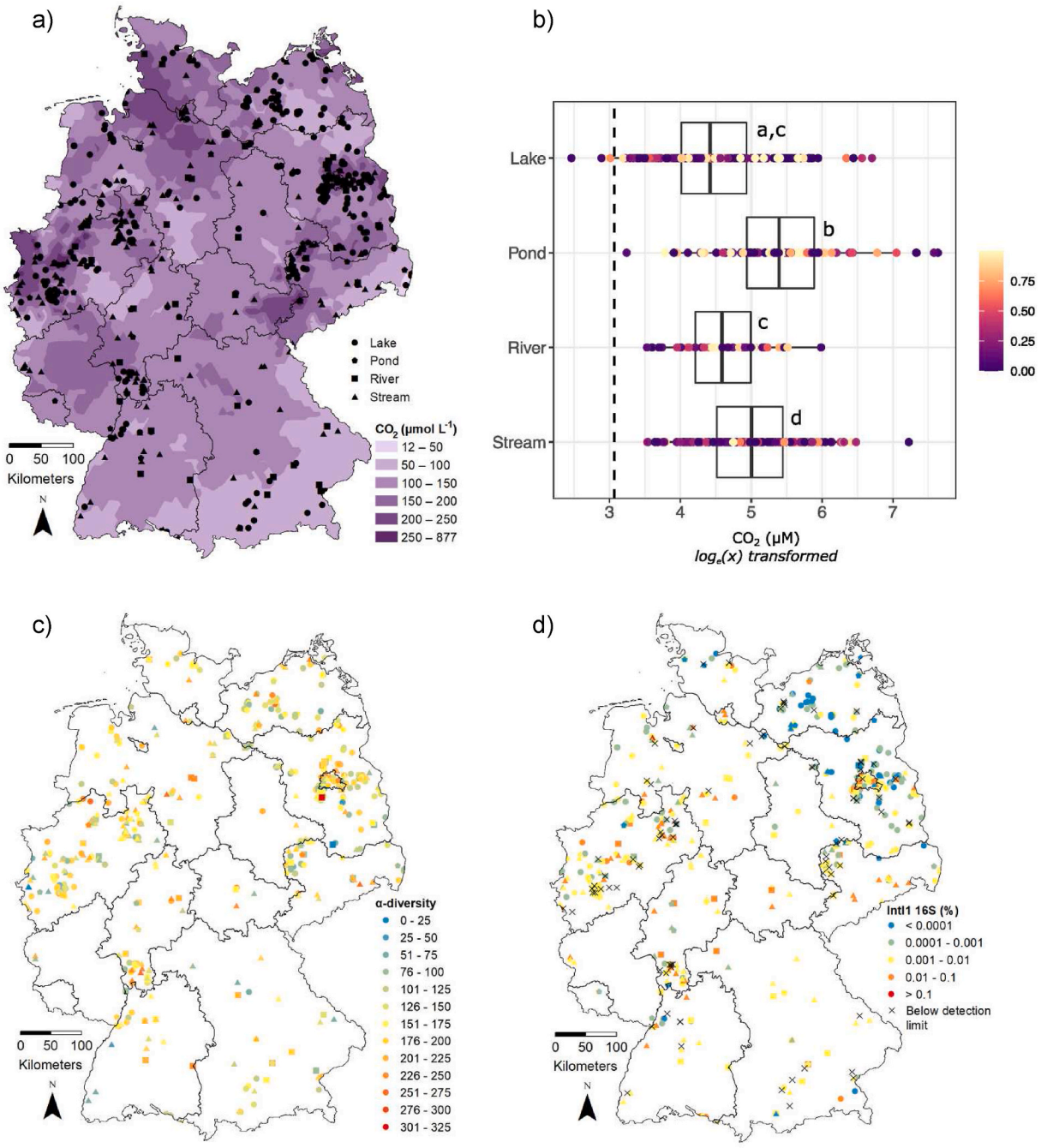

Fig. 1. CO_2 concentrations, microbial diversity, and intI1 abundance in German freshwaters. **a**, Prediction maps of CO_2 concentration in the analysed water bodies across Germany using ordinary kriging. CO_2 values larger than 1000 µmol L^{-1} (n = 6) were excluded from the interpolation. **b**, Measured $\log_{10}$ CO_2 concentrations determined at the different sampling sites according to water body type. Median CO_2 concentration for each water type is displayed as a grey line with the upper and lower limits of the box being the third and first quartile (75th and 25th percentile), respectively. Significant differences in CO_2 concentrations between water types are visualized via distinct letters. The color of each filled circle indicates the proportion of urban landscape in the catchment area of the water body. **c**, Distribution of microbial alpha-diversity. **d**, intI1-gene copy number expressed as the proportion (as %) of 16S rRNA gene copies in the sample. (For interpretation of the references to colour in this figure legend, the reader is referred to the web version of this article.)

individual-taxon correlations (Fig. 4). In particular, Cyanobacteria taxa were negatively correlated with CO_2, and non-phototrophic taxa were positively correlated with CO_2, suggestive of the well described links between both microbial primary and secondary production with CO_2 (Fig. 4). It was surprising that a single point measurement of CO_2 showed such a clear signal in the microbial composition, and suggests that CO_2 is an indicator of different traits in the carbon cycling mediated by the microbial community.

3.2. Light pollution

Using satellite images, we observed that 75% of the sampled water bodies were impacted by artificial light at night based on a threshold radiance of 0.5 nW cm^{-2} sr^{-1}. ALAN was closely connected to urban areas, as expected (Fig. 2), and was significantly higher at river sampling sites than in streams, lakes, and ponds (LM: ALAN ~ waterType * catchment, $R^2 = 0.41$, $F_{3,624} = 9.14$, $P < 0.001$; for River:Urban $\beta = 6.03$, $P = 0.002$), which supports our first hypothesis on light pollution. This

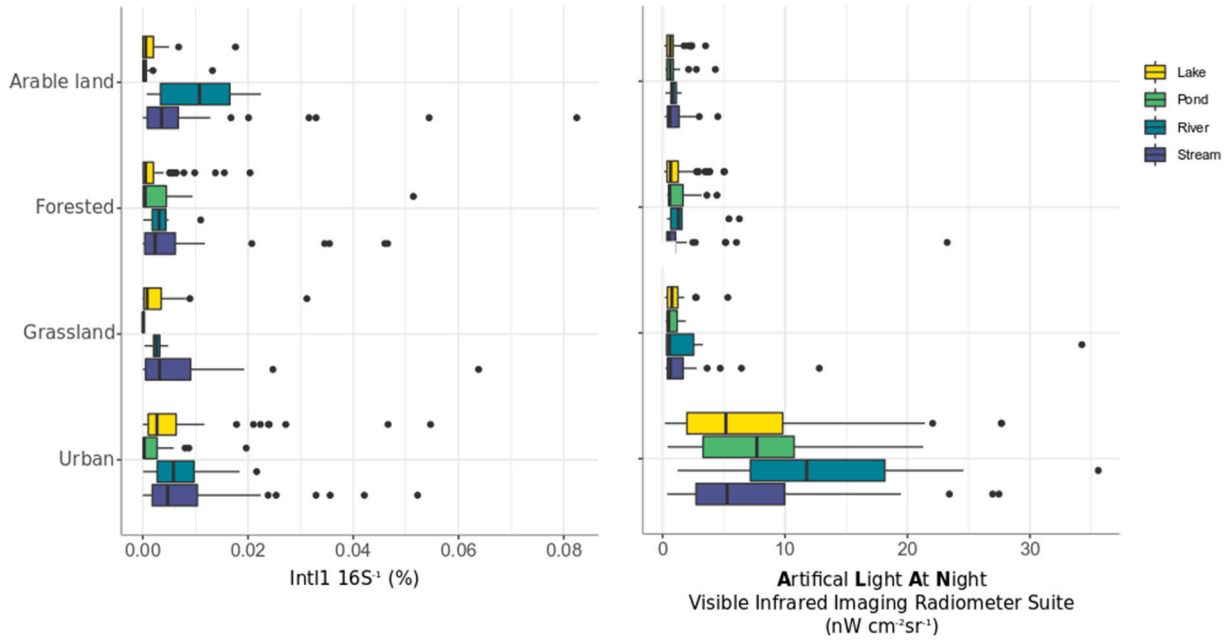

Fig. 2. Pollutant levels by land-use and water-body type. **a,** Relative frequency of the IntI1 gene as a proportion (%) of rRNA gene copies. **b,** Amount of artificial light at night (ALAN) in sampled waters. Box plots separate water types according to the dominant landscape in the catchment area of the sampled water body.

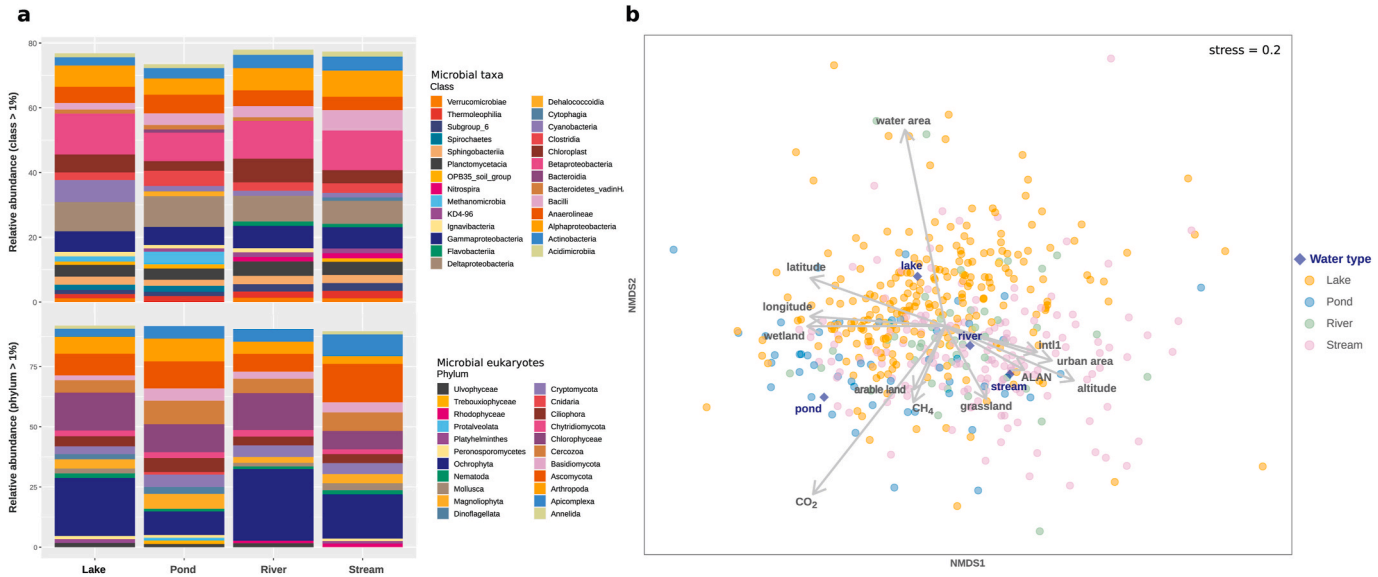

Fig. 3. Freshwater microbiome composition and community relationships to environmental parameters. **a**, Relative abundance of microbial classes (upper panel, all taxa) and phyla (lower panel, microbial eukaryotes) for taxa comprising >1% of total abundance among water-body types. **b**, NMDS summarizing all microbial samples and the corresponding centroids for each water-body type. Environmental parameters were fitted to the plot with individual arrows.

large-scale pattern corroborates a previous study within the city of Berlin, where analysis of aerial photographs revealed that rivers and canals were exposed to six times more ALAN than lakes due to their higher ratio of shoreline to water surface area (Kuechly et al., 2012).

Permutational analysis of variance also confirmed our second hypothesis, that ALAN can influence the structure of the microbial community (Table S3). The overall small effect was strongest in streams and rivers (MCC ~ ALAN: $R^2 = 0.01$, P adjusted $= 0.001$ (Bonferroni)). Interestingly, the interaction of ALAN and CO_2 had no influence on the microbial community (Table S3), which we interpret to mean that the effect of ALAN on microbial communities has not yet resulted in changes to the CO_2, despite experimental evidence for an increase in community respiration due to ALAN (Hölker et al., 2015). This would not directly support our third hypothesis. This lack of a relationship between ALAN and CO_2 was also consistent with there being no effect (LM: CO_2~ ALAN, $R^2 = 0.002$, $F_{1,620} = 1.20$, $P = 0.270$). In contrast to CO_2, we observed no single-taxon correlations of phototrophic bacteria (e.g., Cyanobacteria) with ALAN (Fig. 4, Fig. S3). Our results are partly in agreement with the earlier laboratory study (Hölker et al., 2015) in which the exposure to ALAN led to altered sediment microbial communities. Those communities pre-exposed to ALAN for one year, however, contained more phototrophs being more pronounced during the darker period of the year when temperatures were lower, and the photoperiod was shorter. Together, these results suggest ALAN has implications for ecosystem functions but may not change the carbon balance.

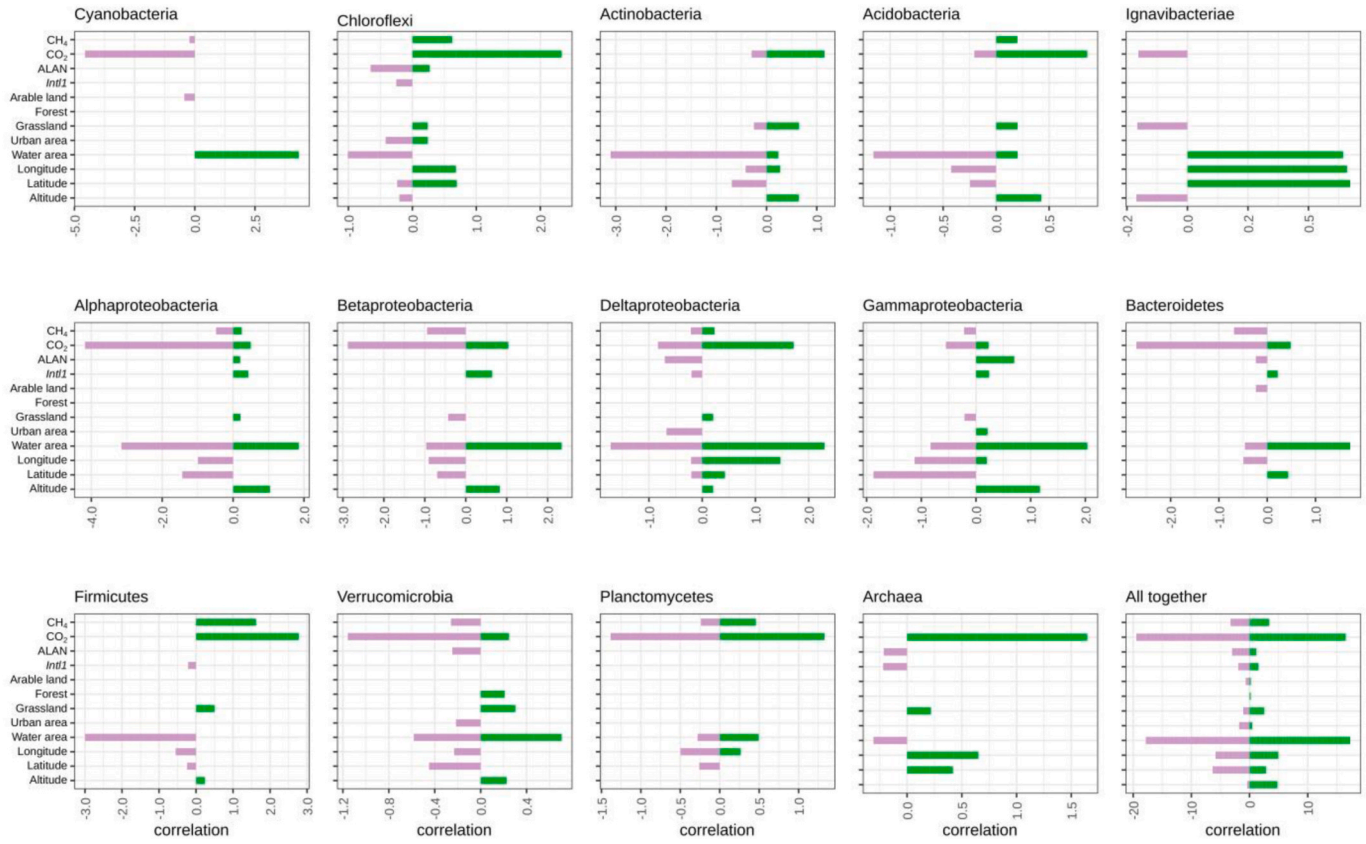

Fig. 4. Correlations between microbial taxa and measured parameters. Cumulative single-species correlations of major microbial taxa with site characteristics and sampled parameters.

3.3. Mobile genetic elements and antibiotic resistances

We used quantitative PCR to measure the presence of the class-1 integron-integrase gene *intI1* and the carbapenem-resistant gene *blaOXA*$_{58}$ as proxies for anthropogenic chemical pollution and anthropogenically induced antimicrobial resistances, respectively (Gillings et al., 2015; Cacace et al., 2019). *IntI1* was detected in 457 of the 541 sites examined (85%) with a median relative abundance of $1.2 * 10^{-5}$ copies per 16S rRNA gene copy. *blaOXA*$_{58}$ was examined in a subset of sites with high *intI1* abundance, as we considered these as anthropogenically impacted sites. In these impacted sites blaOXA58 was detected in 104 of 236 screened sites (44%). Positive correlations of *intI1* and *blaOXA*$_{58}$ occurrence with single taxa of Alphaproteobacteria and Betaproteobacteria (determined through whole-community analysis; see below) suggest that there may be multiple carriers of these genes (Fig. 4, Fig. S4). Our results were similar to findings from other studies of freshwater sediments (Gillings et al., 2015), and clearly indicate that low levels of human-derived microbial resistances are widespread in German freshwaters. *IntI1* prevalence can be linked to agricultural runoff, but we observed it most often in urban areas and in streams and rivers rather than in ponds and lakes (Fig. 2), which does not support our first hypothesis of antimicrobial resistance being pronounced in agricultural areas and suggests instead that urban runoffs and effluents may also be an important source (Gillings, 2015, 2018). In addition to antibiotics, *intI1* has been linked to genes involved in resistance to metals and disinfectants and thus provides a good overall measure of resistance and anthropogenic pollution (Gillings, 2015, 2018). Sampling by citizen scientists may be biased toward waters that are easily accessible and frequently used for recreation, thus the measured gene abundances may be higher than the national average of all water bodies. There was a weak negative relationship with distance to the nearest wastewater treatment plant (known point sources of antibiotic resistance genes) (Cacace et al., 2019) for *intI1* (Spearman's rho = - 0.17, $P < 0.001$) but not for *blaOXA*$_{58}$ ($P > 0.050$), which may be partly explained by samples from directly impacted downstream sites. However, both *intI1* and *blaOXA*$_{58}$ showed highest correlation values with typical lineages that are present in wastewater (vadin BC27), and widespread opportunistic pathogens (*Acinetobacter*) (Gillings, 2018) (Fig. S4).

3.4. Greenhouse gases

Nearly all (>99%) of the sampled water bodies were oversaturated with CO_2, i.e., exceeded that of atmospheric equilibrium indicating that they were net-emitters of CO_2 to the atmosphere at the time of sampling (mornings in early November, Fig. 1). The highest CO_2 concentration was found in ponds (median 218 μmol L^{-1}, interquartile range 140, 361), followed by streams (149 μmol L^{-1}, 91, 231), rivers (98 μmol L^{-1}, 68, 150), and lakes (83 μmol L^{-1}, 55, 138) (Fig. 1b). CH_4 concentrations were also highest in small water bodies and within the expected range based on previous studies. However, in large water bodies, CH_4 concentrations were higher than expected from literature (Holgerson & Raymond, 2016) (Fig. S5). Large-scale patterns in CO_2 showed a weak spatial autocorrelation (Moran's I = 0.09, $P < 0.001$) and a slight increase from low to high latitudes. Such a pattern was not observed for CH_4 concentrations (Table S4; Fig. 1). The pattern in CO_2 may have resulted from a day-length difference of about 45 min from South to North at the sampled sites in November, which fosters respiration and, thus, CO_2 production, during the darker hours. The absence of any large-scale CH_4 pattern can be explained by rapid CH_4 exchange between water and atmosphere, which results in a strong local control on aquatic CH_4.

At smaller scales, CO_2 and CH_4 varied among water body type and land use (Table S4), being highest in ponds and generally higher in urban areas (Fig. 1, Fig. S5). This confirms findings from smaller-scale

studies (Holgerson & Raymond, 2016; Premke et al., 2016) and validates our citizen science approach as a useful tool for synchronous data collection from multiple sites over a wide geographic area. For streams and rivers, we observed a significant increase in CO_2 from low to high latitudes (linear model (LM): $CO_2 \sim$ Stream: $R^2 = 0.21$, $F_{1,203} = 54.89$, $P < 0.001$, $CO_2 \sim$ River: $R^2 = 0.15$, $F_{1,55} = 9.44$, $P = 0.003$) and lower CO_2 in larger streams (LM: $\log10(CO_2) \sim$ Strahler stream order: $F_{9,252} = 4.33$, $R^2 = 0.10$, $P < 0.001$, Fig. S1). Carbonate weathering in the watershed (Marce et al., 2015) can increase carbon export by rivers (Raymond et al., 2008), although this is unlikely to explain the pattern observed because the lithology of northern Germany is carbonate-poor. We propose that higher CO_2 import from the riparian zone, together with lower gas exchange coefficients in lowland streams (Rasilo et al., 2017), were the reason for the latitudinal pattern. These results highlight the complex interaction of natural and anthropogenic factors such as eutrophication and pollution (Beaulieu et al., 2019) in driving GHG concentrations in surface waters.

4. Conclusions

This large-scale citizen-science study allowed for a coordinated sampling campaign of the freshwater surface-sediment microbiome and GHG concentrations in 617 water bodies throughout Germany (357 000 km^2) within a two-week period, something that would not be feasible for a small team of researchers. We conclude that the mobilization of citizen scientists to sample hundreds of sites using standardized methods and within short periods of time is a promising approach for monitoring freshwaters over large areas. Among the more striking findings were that rivers were the aquatic ecosystems most affected by light pollution and where microorganisms were most clearly exhibiting resistance genes that indicate chemical stress and antimicrobial resistance. We observed for the first time in the field that light pollution influences the microbial diversity in freshwater ecosystems, and, although not visible in this snapshot sampling, may potentially affect CO_2 concentrations in the long-term. Interestingly, both anthropogenic stressors had a greater impact on running than on standing water bodies, highlighting the vulnerability of lotic waters. The lower observed impact on pond and lake systems may be related to greater surface areas (and volume) and lower shoreline-to area-ratios. Thus, impacts from outside (e.g., light at the shoreline) and from wastewater or urban areas are therefore lower. Our results provide a basis for better understanding of the influence of anthropogenic stressors on microbial diversity and GHG balance in aquatic ecosystems. Understanding these relationships improves our ability to predict system responses to global climate change, which remains absolutely necessary, given forecast developments in population growth, urbanization, and the unpredictability of the climate.

Credit author statement

K.P., F.H., C.W., and M.T.M. conceived and designed the study. K.P. led the project. K.F. coordinated the project and fieldwork of citizen scientists. K.P. and F.H. first drafted the manuscript and C.W. and M.T.M. contributed to the writing. K.P., F.H., C.W., K.A., J.F., R.T., and S.S. contributed to the interpretation of the data. K.P., K.F., J.F., R.T., K.A., and E.H. organized the sampling campaign and prepared the presampling. K.P., K.F., J.F., R.T., E.H., and M.K. performed the CO_2 and CH_4 concentration measurements which were calculated by P.B. and J.F. C.W. and M.T.M. measured and analysed the microbial DNA metabarcoding data. C.W. and T.H.M. carried out the analysis of *intI-1* and $blaOXA_{58}$ data. C.K. extracted the data on light exposure and elevation from satellite datasets. F.H. and S.S. analysed the light data. E.H. ran the data verification experiment and compiled information on the adjacent landscape (GIS). K.N.N. created the prediction map. C.W., K.N.N., J.F., P.B. and K.A. performed statistical analyses. R.T. provided the German inland waters data set. All authors contributed to the final manuscript.

Declaration of competing interest

The authors declare that they have no known competing financial interests or personal relationships that could have appeared to influence the work reported in this paper.

Data availability

The greenhouse gas data, satellite data, instructions and manuals for the citizens, and all in-situ derived temperature and pH data can be accessed at the supplementary material. All sequenced amplicon data for this study and their raw reads are available from European Nucleotide Archive (ENA, https://www.ebi.ac.uk/ena/browser/home, PRJEB53570). All data that support the findings of this study are available from the corresponding author on request as well. Code and R scripts used to analyse the data are available on Github except for analyses where all settings are fully reported in the Methods.

Acknowledgments

We gratefully acknowledge the participation of the 742 citizen scientists and groups throughout Germany who carefully and conscientiously sampled water and sediment samples, in many cases of their favourite water body, and provided information about ALAN. The project could not have been carried out without their help. We thank J. Oestmann, S. Heller, and E. N. De Nardi for their practical support in the preparation and execution of the analyses and creating the youtube video, J. Mahnkopf for GIS advice and fruitful discussions, and A. Entin for calculating the Strahler stream orders. We thank C. Weiβenborn for performing DNA extractions and PCRs, S. Sparmann and S. Mbedi at the Berlin Center for Genomics in Biodiversity Research for library preparation and next-generation sequencing, and A. Nawaz for sequence data processing. We thank the environmental authorities from the federal states of Germany for providing basic data on lakes. We thank the three anonymous reviewers for their constructive inputs which improved the manuscript.

Appendix A. Supplementary data

Supplementary data to this article can be found online at https://doi.org/10.1016/j.envpol.2022.119627.

References

AKTIS, 2013. Authorative Topographic-Cartographic Information System (ATKIS®) Data Set. © GeoBasis-DE/German Federal Agency for Cartography and Geodesy - BKG.
Amos, G.C.A., Zhang, L., Hawkey, P.M., Gaze, W.H., Wellington, E.M., 2014. Functional metagenomic analysis reveals rivers are a reservoir for diverse antibiotic resistance genes. Vet. Microbiol. 171, 441–447.
Attermeyer, K., et al., 2016. Invasive floating macrophytes reduce greenhouse gas emissions from a small tropical lake. Sci. Rep. 6, 20424.
Aufdenkampe, A.K., et al., 2011. Riverine coupling of biogeochemical cycles between land, oceans, and atmosphere. Front. Ecol. Environ. 9, 53–60.
Baird, A.J., Stamp, I., Heppell, C.M., Green, S.M., 2010. CH4 flux from peatlands: a new measurement method. Ecohydrology 3, 360–367.
Bakke, I., De Schryver, P., Boon, N., Vadstein, O., 2011. PCR-based community structure studies of Bacteria associated with eukaryotic organisms: a simple PCR strategy to avoid co-amplification of eukaryotic DNA. J. Microbiol. Methods 84, 349–351.
Barraud, O., Baclet, M.C., Denis, F., Ploy, M.C., 2010. Quantitative multiplex real-time PCR for detecting class 1, 2 and 3 integrons. J. Antimicrob. Chemother. 65, 1642–1645.
Bates, D., Mächler, M., Bolker, B., Walker, S., 2015. Fitting linear mixed-effects models using lme4. J. Stat. Software 67 (1), 1–48. https://doi.org/10.18637/jss.v067.i01.
Beaulieu, J.J., DelSontro, T., Downing, J.A., 2019. Eutrophication will increase methane emissions from lakes and impoundments during the 21st century. Nat. Commun. 10, 1375.
Bengtsson-Palme, J., Larsson, D.G.J., 2015. Antibiotic resistance genes in the environment: prioritizing risks. Nat. Rev. Microbiol. 13, 396.
Bolger, A.M., Lohse, M., Usadel, B., 2014. Trimmomatic: a flexible trimmer for Illumina sequence data. Bioinformatics 30, 2114–2120.

Bretz, K.A., et al., 2021. Integrating ecosystem patch contributions to stream corridor carbon dioxide and methane fluxes. J. Geophys. Res.: Biogeosciences 126, e2021JG006313. https://doi.org/10.1029/2021JG006313.
Cacace, D., et al., 2019. Antibiotic resistance genes in treated wastewater and in the receiving water bodies: a pan-European survey of urban settings. Water Res. 162, 320–330.
Cavicchioli, R., et al., 2019. Scientists' warning to humanity: microorganisms and climate change. Nat. Rev. Microbiol. 17, 569–586.
Conrad, O., et al., 2015. System for automated geoscientific analyses (SAGA) v. 2.1.4. Geosci. Model Develop 8, 1991–2007.
Crevecoeur, S., Ruiz-Gonzalez, C., Prairie, Y.T., del Giorgio, P.A., 2019. Large-scale biogeography and environmental regulation of methanotrophic bacteria across boreal inland waters. Mol. Ecol. 28, 4181–4196.
da Silva, G.V.R., Castañeda-Ruiz, R.F., Malosso, E., 2019. Comparison of aquatic hyphomycetes communities between lotic and lentic environments in the Atlantic rain forest of Pernambuco, Northeast Brazil. Fungal Biol. 123 (9), 660–668.
del Giorgio, P.A., Duarte, C.M., 2002. Respiration in the open ocean. Nature 420, 379–384.
Drake, T.W., Raymond, P.A., Spencer, R.G.M., 2018. Terrestrial carbon inputs to inland waters: a current synthesis of estimates and uncertainty. Limnol. Oceanogr. Lett. 3, 132–142.
Ernst, L., Steinfeld, B., Barayeu, U., et al., 2022. Methane formation driven by reactive oxygen species across all living organisms. Nature 603, 482–487. https://doi.org/10.1038/s41586-022-04511-9.
Gillings, M.R., 2018. DNA as a pollutant: the clinical class 1 integron. Curr. Poll. Rep. 4, 49–55.
Gillings, M.R., et al., 2015. Using the class 1 integron-integrase gene as a proxy for anthropogenic pollution. ISME J. 9, 1269–1279.
Grubisic, M., et al., 2017. Artificial light at night decreases biomass and alters community composition of benthic primary producers in a sub-alpine stream. Limnol. Oceanogr. 62, 2799–2810.
Gudasz, C., et al., 2010. Temperature-controlled organic carbon mineralization in lake sediments. Nature 466, 478-U473.
Han, X.G., Schubert, C.J., Fiskal, A., Dubois, N., Lever, M.A., 2020. Eutrophication as a driver of microbial community structure in lake sediments. Environ. Microbiol. 22, 3446–3462.
Holgerson, M.A., Raymond, P.A., 2016. Large contribution to inland water CO2 and CH4 emissions from very small ponds. Nat. Geosci. 9, 222-U150.
Hölker, F., et al., 2015. Microbial diversity and community respiration in freshwater sediments influenced by artificial light at night. Phil. Trans. R. Soc. B- 370, 20140130.
Hölker, F., et al., 2010. The dark side of light: a transdisciplinary research agenda for light pollution policy. Ecol. Soc. 15, 13.
Hölker, F., Bolliger, J., Davies, T.W., Giavi, S., Jechow, A., Kalinkat, G., Longcore, T., Spoelstra, K., Tidau, S., Visser, M.E., Knop, E., 2021. 11 pressing research questions on how light pollution affects biodiversity. Front. Ecol. Evol. 9, 767177.
Hsieh, T.C., Ma, K.H., Chao, A., 2016. iNEXT: an R package for rarefaction and extrapolation of species diversity (Hill numbers). Meth. Ecol. Evol. 7, 1451–1456.
Jechow, A., Hölker, F., 2019. How dark is a river? Artificial light at night in aquatic systems and the need for comprehensive night-time light measurements. Wiley Interdisciplin. Rev.: Water 6, e1388.
Kling, G.W., Kipphut, G.W., Miller, M.C., 1991. Arctic lakes and streams as gas conduits to the atmosphere - implications for Tundra carbon budget. Science 251, 298–301.
Kuechly, H.U., et al., 2012. Aerial survey and spatial analysis of sources of light pollution in Berlin, Germany. Rem. Sens. Environ. 126, 39–50.
Kyba, C.C.M., et al., 2017. Artificially lit surface of Earth at night increasing in radiance and extent. Sci. Adv. 3, e1701528.
Kyba, C.C.M., et al., 2013. Citizen science provides valuable data for monitoring global night sky luminance. Sci. Rep. 3, 1835.
Lagkouvardos, I., Fischer, S., Kumar, N., Clavel, T., 2017. Rhea: a transparent and modular R pipeline for microbial profiling based on 16S rRNA gene amplicons. PeerJ 5, e2836.
Lehner, B., Verdin, K., Jarvis, A., 2008. New global hydrography derived from spaceborne elevation data. Transact. Amer. Geophys. 89, 93–104.
Liaw, A., Wiener, M., 2002. Classification and regression by randomForest. R. News 2, 18–22.
Liguori, R., Rommel, S.H., Bengtsson-Palme, J., Helmreich, B., Wurzbacher, C., 2021. Microbial retention and resistances in stormwater quality improvement devices treating road runoff. FEMS Microb. 2 https://doi.org/10.1093/femsmc/xtab008.
Lima, T., et al., 2020. Manure as a potential hotspot for antibiotic resistance dissemination by horizontal gene transfer events. Vet Sci 7 (3), 110.
Manfrin, A., et al., 2017. Artificial light at night affects organism flux across ecosystem boundaries and drives community structure in the recipient ecosystem. Front. Environ. Sci. 5, 61.
Marce, R., et al., 2015. Carbonate weathering as a driver of CO2 supersaturation in lakes. Nat. Geosci. 8, 107–111.
McMurdie, P.J., Holmes, S., 2013. Phyloseq: an R package for reproducible interactive analysis and graphics of microbiome census data. PLoS One 8, e61217.
Nawaz, A., et al., 2018. First insights into the living groundwater mycobiome of the terrestrial biogeosphere. Water Res. 145, 50–61.
Oksanen, J., Kindt, R., Legendre, P., O'Hara, B., Stevens, M.H.H., Oksanen, M.J., et al., 2007. The Vegan Package, 10. Commun. Ecol. Packag, p. 719 https://CRAN.R-project.org/package=vegan.
OpenStreetMap, 2018. SRTM digital terrain model of Germany. Access date 12 October 2018. Derived from SRTM and OSM data.
Premke, K., et al., 2016. The importance of landscape diversity for carbon fluxes on the landscape level: small-scale heterogeneity matters. WIREs Wat 12, 1354.
Pruim, R., Kaplan, D.T., Horton, N.J., 2017. The mosaic package: helping students to 'think with data' using R. R J. 9, 77–102.
Quast, C., et al., 2013. The SILVA ribosomal RNA gene database project: improved data processing and web-based tools. Nucleic Acids Res. 41, D590–D596.
R Core Team, R., 2018. A Language and Environment for Statistical Computing. R Found. Stat. Comput. Vienna, Austria.
Rasilo, T., Hutchins, R.H.S., Ruiz-Gonzalez, C., del Giorgio, P.A., 2017. Transport and transformation of soil-derived CO_2, CH_4 and DOC sustain CO_2 supersaturation in small boreal streams. Sci. Total Environ. 579, 902–912.
Raymond, P.A., et al., 2013. Global carbon dioxide emissions from inland waters. Nature 503, 355–359.
Raymond, P.A., Oh, N.H., Turner, R.E., Broussard, W., 2008. Anthropogenically enhanced fluxes of water and carbon from the Mississippi River. Nature 451, 449–452.
Regnier, P., et al., 2013. Anthropogenic perturbation of the carbon fluxes from land to ocean. Nat. Geosci. 6, 597–607.
Reid, A.J., et al., 2019. Emerging threats and persistent conservation challenges for freshwater biodiversity. Biol. Rev. 94, 849–873.
Reynolds, C.S., Descy, J.P., Padisák, J., 1994. Are phytoplankton dynamics in rivers so different from those in shallow lakes? Hydrobiologia 289, 1–7. https://doi.org/10.1007/BF00007404.
Salter, S.J., et al., 2014. Reagent and laboratory contamination can critically impact sequence-based microbiome analyses. BMC Biol. 12, 87.
Sander, R., 1999. Compilation of henry's law constants for inorganic and organic species of potential importance. Environ. Chem.
Schroer, S., et al., 2016. The impact of outdoor lighting on ecosystem function–gaining information with a Citizen Science approach using a questionnaire. Front. Environ. Sci. https://doi.org/10.3389/conf.FENVS.
Tranvik, L.J., et al., 2009. Lakes and reservoirs as regulators of carbon cycling and climate. Limnol. Oceanogr. 54, 2298–2314.
Veach, A.M., Troia, M.J., Cregger, M.A., 2021. Assessing biogeographic survey gaps in bacterial diversity knowledge: A global synthesis of freshwaters. Freshw. Biol. 66 (8), 1595–1605.
Venohr, M., et al., 2018. The underestimated dynamics and impacts of water-based recreational activities on freshwater ecosystems. Environ. Rev. 26 (2), 199–213.
Verburg, P.H., et al., 2016. Methods and approaches to modelling the Anthropocene. Global Environ. Change 39, 328–340.
Villanueva, R.A.M., Chen, Z.J., 2019. ggplot2: elegant graphics for data analysis. Meas. Interdisc. Res. Persp. 17, 160–167 second ed.
Wan, Y., Ruan, X.H., Zhang, Y.P., Li, R.F., 2017. Illumina sequencing-based analysis of sediment bacteria community in different trophic status freshwater lakes. Microbiol. open 6, e00450.
Whitman, W.B., Coleman, D.C., Wiebe, W.J., 1998. Prokaryotes: the unseen majority. Proc. Natl. Acad. Sci. U.S.A. 95, 6578–6583.
Wilkinson, J., Bors, C., Burgis, F., Lorke, A., Bodmer, P., 2019. Measuring CO2 and CH4 with a portable gas analyzer: closed-loop operation, optimization and assessment. PLoS One 14, e0206080.
Wurzbacher, C., et al., 2017. DNA metabarcoding of unfractionated water samples relates phyto-, zoo- and bacterioplankton dynamics and reveals a single-taxon bacterial bloom. Environ. Microbiol. Rep. 9, 383–388.
Zhang, J.J., Kobert, K., Flouri, T., Stamatakis, A., 2014. PEAR: a fast and accurate Illumina Paired-End reAd mergeR. Bioinformatics 30, 614–620.